RSC Advances

PAPER

View Article Online
View Journal | View Issue

Cite this: *RSC Adv.*, 2023, **13**, 33288

Development of an automated Raman system and use of principal component analysis to classify real and counterfeit liquors†

Huan-Wen Chi, Shu-Wei Hu and Ding-Zheng Lin *

Received 5th September 2023
Accepted 27th October 2023

DOI: 10.1039/d3ra06057h

rsc.li/rsc-advances

We developed an automated Raman measurement platform for the customized design of various solution containers. We used the software LabVIEW to integrate the entire automatic measurement process. By designing an intuitive human–machine interface, the user only needs to input a few setting parameters and can efficiently operate the machine in automation mode for an array of solutions containing real or counterfeit liquors such as kaoliang liquor, vodka, rum, gin, rice wine, ethanol, and methanol. In this study, data from various alcoholic beverage solutions were subjected to principal component analysis (PCA) to distinguish from the low-concentration counterfeit liquors (methanol <50 g L^{-1}). Moreover, several brands of liquors with the same alcohol concentration were successfully classified into different groups based on a combination of Raman spectroscopy and PCA analysis.

1. Introduction

Foodborne illness outbreaks have occurred in recent years, such as that from using industrial alcohol to brew wine in Taiwan in 2008, the plasticizer incident in 2011,[1] and the fipronil egg incident in 2017.[2,3] Those incidents panicked consumers and raised awareness of food safety. Thus, optical detection should be applied to food safety and regulation to reduce the risk of consuming unsafe food and improve the competitiveness of the food industry. Raman spectroscopy is one of the few technical methods that can rapidly, sensitively, nondestructively, and inexpensively detect essentially all pollutants. The Raman spectroscopy does not demand excessive pretreatment, the appearance, and phase of the sample. Compared with other spectroscopy methods (*e.g.*, photoluminescence spectroscopy and electroluminescence spectroscopy), Raman spectroscopy offers a higher spectral resolution and narrower bandwidth for analyzing multiple subjects.[4]

Alcoholic beverages are complicated mixtures with the components mainly being ethanol and water, as well as volatile compounds that are mainly responsible for the smell and flavor of the beverage. Currently, alcoholic beverages can be divided into two types: fermented alcoholic beverages and liquor. Methanol, also known as industrial alcohol, is highly harmful to humans. In human metabolism, methanol oxidizes to the more toxic formaldehyde and formic acid, which can cause headaches, dizziness, fatigue, nausea, vomiting, blurred vision, and even blindness or death. Despite these dangers, many unscrupulous merchants still disregard human safety and use methanol to adulterate counterfeit liquor and sell it. However, many liquor products contain trace amounts of methanol because it is produced to some extent during the fermentation process of making liquor.[5] From 1979 to 2008, there were frequent incidents involving counterfeit liquor in Taiwan, with industrial alcohol being the primary source. There have also been cases of counterfeit alcohol since 2008; however, almost all were unrelated to industrial alcohol and involving processes such as using detergents to make plum wine and using coloring and inferior wine mixes to make counterfeit wine. Although industrial-alcohol production is almost nonexistent in Taiwan today, it can still be found in India, Iran, Russia, and some developing countries.[6,7]

Recently, there has been much literature focused on the application of Raman spectroscopy/surface-enhanced Raman spectroscopy (SERS) to fruit,[8] milk,[9] and the environment[10,11] but only a few studies on distinguishing the brands of commercial liquors using analytical methods.[12,13] Therefore, in this research, we developed an automated system for determining alcohol concentration and brand type through Raman spectroscopy. First, we quantified the alcohol concentration according to the intensities of ethanol Raman peaks. Then, we analyzed counterfeit liquors and applied principal component analysis (PCA) to investigate the Raman spectral differences between ethanol and methanol mixtures. Furthermore, we achieved the successful classification of different commercial liquor brands using PCA. The determination of alcohol concentration was facilitated through the analysis of Raman spectra or by identifying the nearest group in the PCA diagram based on different ethanol concentration standards.

Department of Mechanical Engineering, National Taiwan University of Science and Technology, Taipei, Taiwan. E-mail: djsam@mail.ntust.edu.tw

† Electronic supplementary information (ESI) available. See DOI: https://doi.org/10.1039/d3ra06057h

2. Materials and methods

The architecture of our automation Raman system is referenced from the conventional Raman system, as well as the optical system schematic and the scattering optical path of the optical elements of the Raman chemical automated imaging system by Jianwei Qin *et al.*[14] A diagram of the architecture of the automated Raman system is shown in Fig. 1. The system hardware included a 532 nm-wavelength laser, a spectrometer, a CCD camera, a stepper motor, a microcontroller evaluation board (STM32, F302R8), a micro stepper motor driver board (STM32, L6470), and some optical components. The 532 nm-wavelength laser, generated from a source with 200 mW input power, was passed through a laser cleanup filter (Semrock, LL01-532-12.5) first to form pure 532 nm-wavelength light and was reflected downward using a dichroic mirror (Semrock, LPD02-532RU-25x36x1.1). The laser was then focused on the test sample by deploying a 20× objective lens for Raman spectrum excitation. The Raman scattered light was collected using the same objective lens, with longer wavelengths of light then passing through the dichroic mirror, designed to filter out the Rayleigh scattered light. Moreover, the scattered light from the sample was filtered out again using another high-quality long-pass filter (Semrock, LP03-532RU-25) to eliminate the excitation laser. A beam splitter with a reflectance to transmittance ratio of 10 : 90 was placed in the light path to share 10% of the reflected light for the CCD camera. The position of the laser spot on the sample was clearly observed when using the CCD camera. The remaining 90% of the light was passed through the achromatic lens (Thorlabs, AC254-030A) and was focused onto the optical fiber to the spectrometer (BWTEK, BTC661E) for spectral analysis. The integration time for each spectrum was 1 s. Moreover, each spectrum was the average of three collections to ensure representative sampling and a good signal-to-noise ratio, as the liquor samples lack a significant fluorescence background. Here, we chose a 532 nm-wavelength laser based on the consideration of a higher Raman scattering cross-section, which can more effectively excite molecular vibration modes in alcohol samples, yielding a stronger Raman signal. This choice helped improve the signal-to-noise ratio, enabling the detection of weaker signals or increased sensitivity to lower-concentration alcohol samples.

Additionally, to successfully collect data from the alcohol solutions, we made a bottle holder that was mainly used to place wine bottles and ensure that the bottles were fixed during platform movement and measurement. The bottle holder can hold three bottles each with dimensions of 34 mm × 11.6 mm. The holder was made of polylactic acid (PLA) using a 3D printer and fixed on the motorized *X*–*Y* platform, as shown in Fig. 2(a). A schematic of the nine-point dot-matrix scanning path followed is shown in Fig. 2(b).

The software of the automated Raman system was built by NI LabVIEW to integrate the entire automation measurement process. The human–machine interface of the automated Raman measurement system can be divided into six areas: Raman spectroscopy signal graph, real-time image, parameters

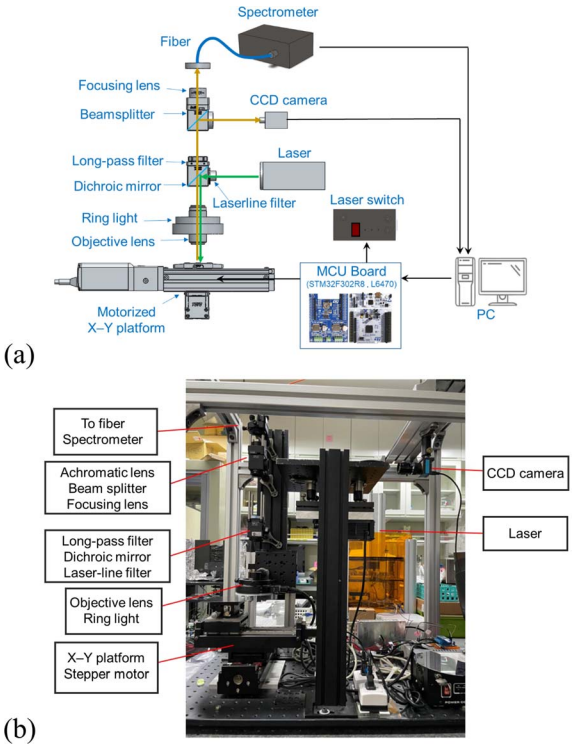

Fig. 1 (a) Schematic diagram and (b) photograph of the automated Raman system involving 532 nm-wavelength light.

of the spectrometer, parameters of motor control, parameters of the camera, and action icons, as shown in Fig. S1(a).† The measurement flow chart is shown in Fig. S1(b).†

First, we acquired the standard curves of methanol and ethanol solutions. A solution of 99.8% ethanol (or 95% methanol) was diluted to 90%, 80%, 70%, 60%, 50%, 40%, 30%, 20% and 10% using distilled water. Second, we blended a commercially available vodka with industrial alcohol to mimic counterfeit distilled liquor. In the past, industrial alcohol has been detected in such commercially available liquor.[15] According to the regulations of the Laws & Regulations of the Republic of China, the amount of methanol in distilled spirits must be <4000 mg L^{-1}, hence defining any such spirit containing >4000 mg L^{-1} as a counterfeit distilled liquor. The commercially available vodka and 95% methanol concentrations were blended into different concentrations, including 0, 5000, 10 000, 50 000, 100 000, and 200 000 mg L^{-1}. The 0 mg L^{-1} represented the pure commercially

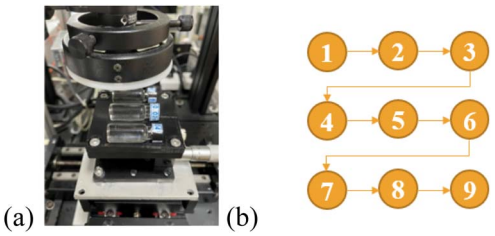

Fig. 2 (a) Photograph of the bottle holder used to place wine bottles, and (b) schematic of the scanning path involving nine points.

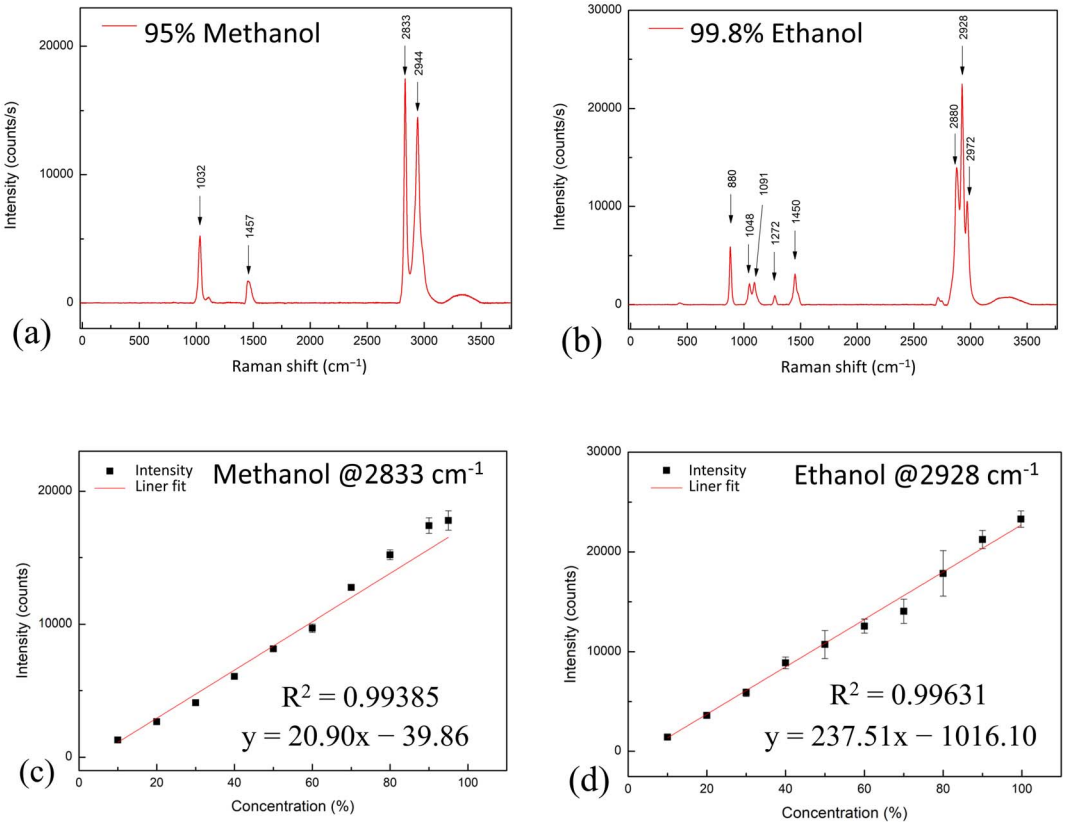

Fig. 3 Raman spectrum of (a) methanol and (b) ethanol, and the concentration curve of (c) methanol and (d) ethanol.

available vodka, whereas the others represented counterfeit distilled liquor. Finally, we analyzed rice cooking wine (Michiu) and distilled liquors of various concentrations, as shown in Table S1.† Round glass jars each with a volume of 1.8 mL were filled with their respective alcohol solutions, specifically filled up all the way to prevent the formation of air bubbles and hence avoid focusing errors in the measurements resulting from the different refractive indexes of air, glass, and liquor solutions. Each bottle, after being filled with the solution, was placed on a bottle holder for automated measurement, as shown in Fig. 2(a).

3. Results and discussion

3.1 Methanol and ethanol standard concentration curves

The Raman spectra of the 95% methanol and 99.8% ethanol solutions are shown in Fig. 3(a) and (b). The corresponding Raman peaks are summarized in Tables S2 and S3† indicate the molecular vibrations and Raman shifts of methanol and ethanol.[16–18] The concentration curves acquired by analyzing 2833 cm^{-1} methanol Raman peaks and 2928 cm^{-1} ethanol Raman peaks are shown in Fig. 3(c) and (d). The

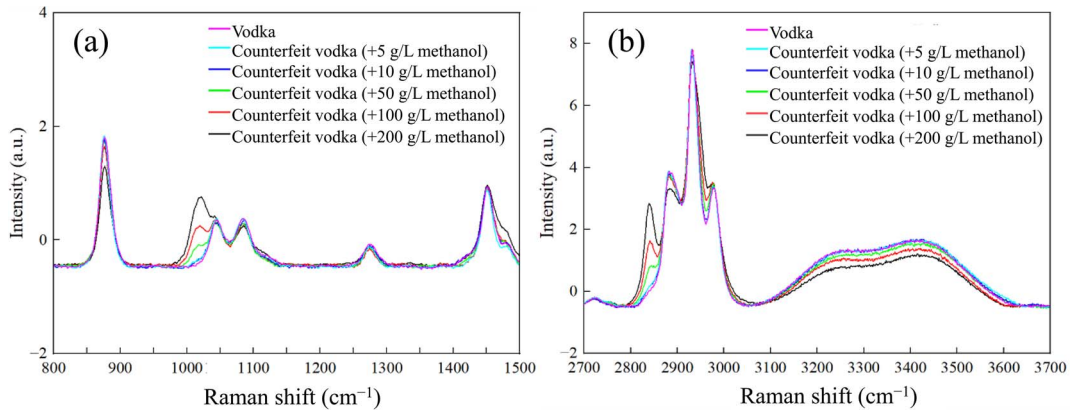

Fig. 4 Raman spectra of counterfeit liquor and commercially available liquor vodkas at various concentrations in the (a) low-Raman-shift region and (b) high-Raman-shift region.

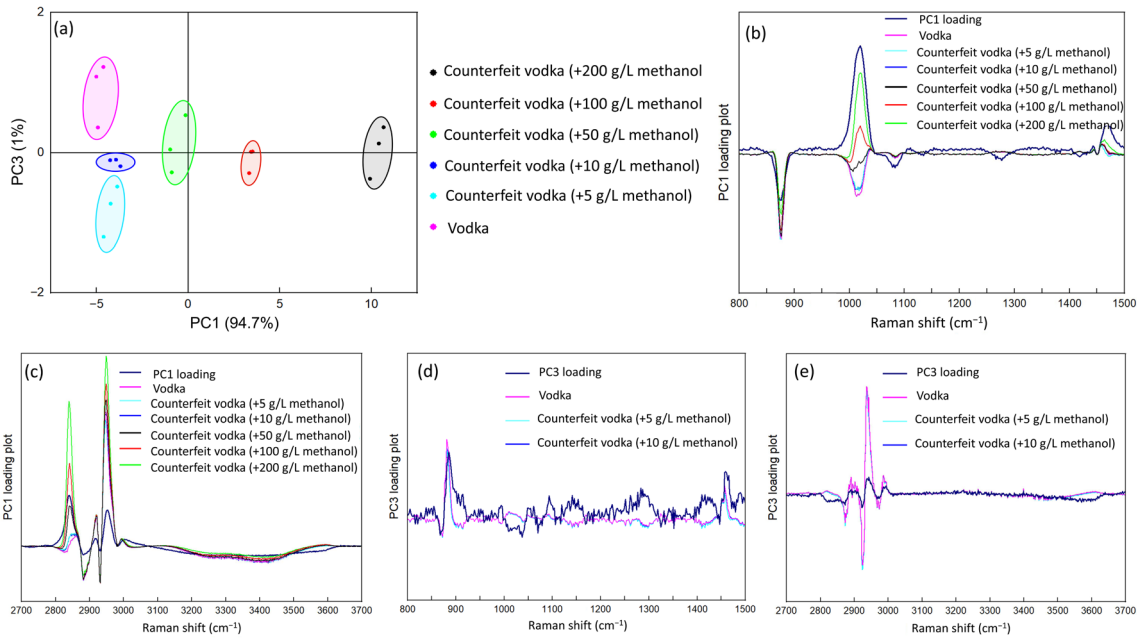

Fig. 5 (a) PCA of Raman spectra of real and counterfeit vodkas based on PC1 and PC3 projections. (b and c) PC1 loading plots of (b) low and (c) high Raman shifts. (d and e) PC3 loading plots of (d) low and (e) high Raman shifts.

concentration curves each produced using data from a different Raman peak, for each of the Raman peaks, are shown in Fig. S2 and S3.† These measurement results showed this procedure to be helpful for the quantitative measurement of methanol (or ethanol) concentration, specifically due to the excellent linearity of the regression line with a coefficient of determination >0.99 ($R^2 > 0.994$).

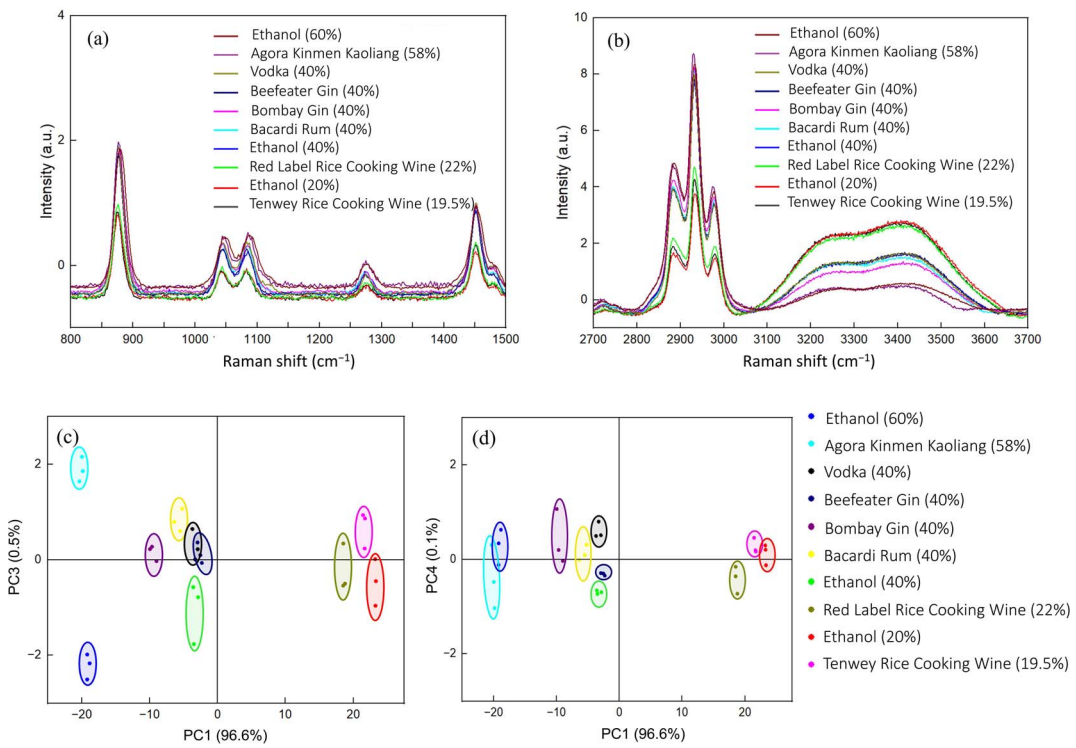

Fig. 6 (a and b) Raman spectra at (a) low and (b) high Raman shifts of indicated commercially available liquors. (c) PC1–PC3 axes and (d) PC1–PC4 axes of PCA plots of indicated brands of commercial liquors.

3.2 Classification of counterfeit liquors

We used the automated Raman system to collect data from the prepared counterfeit liquors. A comparison of the spectra is shown in Fig. 4. Raman peaks of methanol were observed at 1032, 2833, and 2944 cm^{-1} for samples with high concentrations (200, 100, and 50 g L^{-1}); however, they were not clearly distinguished from vodka at lower concentrations (5 and 10 g L^{-1}). Nevertheless, due to the lower concentrations still being >4000 mg L^{-1} and hence considered counterfeit liquors based on the Laws & Regulations of the Republic of China, we attempted to use the PCA method to further discriminate between counterfeit liquors at low concentrations. We performed PCA analysis using Originlab2022 for spectral data preprocessing. Initially, background subtraction was applied to the spectra, followed by data standardization. The PCA was conducted using the PCA package in Originlab2022, resulting in the generation of the PCA plot shown in Fig. 5.

As shown in Fig. 5, PCA allowed for absolute vodka to be differentiated from the low-concentration counterfeit vodkas. Loading plots were obtained by multiplying the PC1 and PC3 weights with the original spectral data obtained from the Raman spectral data projected onto each principal component axis as shown in Fig. 5(b)–(e). The principal components of the characteristic peaks (PC1) comprised partially methanol and partially ethanol. The PC1 variances were related to the concentration of methanol in counterfeit vodka. Moreover, low-concentration counterfeit vodka was further distinguished by the PC3 variances, which were based on some nonobvious characteristic features, making for a more delicate classification.

3.3 Classification of commercially available liquors

Finally, we acquired the Raman spectra of seven commercially available liquors and three concentrations of ethanol (20%, 40%, and 60%), and the results are shown in Fig. 6(a) and (b). We found the significant Raman peaks to be consistent with ethanol, with the peak strength being related to the alcohol concentration. However, a little bit of difference was identified between different brands of liquors. Therefore, we also deployed PCA to analyze these Raman spectra. As shown in Fig. 6(c) and (d), we found three groups along the PC1 axis, which reflects the concentration of alcohol (20%, 40%, and 60%). Moreover, the minor differences between the alcohol brands were successfully determined using the PC3 or PC4 axis.

4. Conclusions

Analysis of the standard concentration curves of the Raman spectra of ethanol and methanol showed excellent-for-quantification R^2 values >0.99 for each characteristic peak. The difference between real liquors and high-concentration counterfeit liquors (containing methanol >50 g L^{-1}) can be determined using Raman spectroscopy. However, at lower concentrations of counterfeit liquors, PCA must be further used for accurate differentiations. The weights of the principal components can be multiplied by their original spectral data to determine the characteristic features of each principal component. We also successfully classified different brands of commercial liquors using PCA, and both Raman spectra and the closest group in the PCA diagram by ethanol standards of different concentrations can be used to determine the alcohol concentration. The data showed that the classification results were accurate, and this analysis method can be extended to other fields, such as food,[19] the environment,[20] and cellular discrimination,[21] and can even be combined with advanced SERS techniques for performing trace contaminant analysis.

Conflicts of interest

There are no conflicts to declare.

Acknowledgements

This work was financially supported by the National Science and Technology Council (MOST 111-2221-E-011-123-MY2), Taiwan. Moreover, we sincerely appreciate the technical guidance from Professor J. K. Wang at the Institute of Atomic and Molecular Sciences, Academia Sinica.

References

1 J.-H. Li and Y.-C. Ko, *Kaohsiung J. Med. Sci.*, 2012, **28**, S17–S21.
2 S. S. Cheng and P.-C. Chuang, *SAGE Open*, 2022, **12**, 215824402210788.
3 H. L. Lai, S. Ghosh and S. Chattopadhyay, *Analyst*, 2021, **146**, 3557–3567.
4 J. R. Ferraro, K. Nakamoto and C. W. Brown, *Introductory Raman spectroscopy*, Academic Press, Amsterdam, Boston, 2nd edn, 2003.
5 International Agency for Research on Cancer and International Agency for Research on Cancer, *Alcohol drinking: views and expert opinions: this publication represents the views and expert opinions of an IARC Working Group on the Evaluation of the Carcinogenic Risk of Chemicals to Humans which met in Lyon, 13–20 October 1987*, International Agency for Research on Cancer, Lyon, 1988.
6 R. Solgi, L. Taheri-Kamalan, A. Larki-Harchegani and A. Nili-Ahmadabadi, *Forensic Toxicol.*, 2021, **39**, 518–521.
7 Y. Solodun, Y. Monakhova, T. Kuballa, A. Samokhvalov, J. Rehm and D. Lachenmeier, *Interdiscip. Toxicol.*, 2011, **4**, 198–205.
8 C. Berghian-Grosan and D. A. Magdas, *Sci. Rep.*, 2020, **10**, 21152.
9 B. Lee, D. Lin, C. Huang and T. Yen, *J. Raman Spectrosc.*, 2018, **49**, 1920–1927.
10 D. Z. Lin, Y. P. Chen, P. J. Jhuang, J. Y. Chu, J. T. Yeh and J.-K. Wang, *Opt. Express*, 2011, **19**, 4337.
11 B.-S. Lee, P.-C. Lin, D.-Z. Lin and T.-J. Yen, *Sci. Rep.*, 2018, **8**, 516.
12 A. Nose, M. Myojin, M. Hojo, T. Ueda and T. Okuda, *J. Biosci. Bioeng.*, 2005, **99**, 493–501.

13 Y. Wu, W. Yu, B. Yang and P. Li, *Analyst*, 2018, **143**, 2363–2368.
14 J. Qin, K. Chao and M. S. Kim, *Trans. ASABE*, 2010, **53**, 1873–1882.
15 M. A. Khodasevich, G. V. Sinitsyn, M. A. Gres'ko, V. M. Dolya, M. V. Rogovaya and A. V. Kazberuk, *J. Appl. Spectrosc.*, 2017, **84**, 517–520.
16 A. Emin, A. Hushur and T. Mamtimin, *AIP Adv.*, 2020, **10**, 065330.
17 H. Vašková and M. Tomeček, *MATEC Web Conf.*, 2018, **210**, 02035.
18 H. Vaskova, *Int. J. Biol. Biomed. Eng.*, 2014, **8**, 27–34.
19 L. Li, X. Cao, T. Zhang, Q. Wu, P. Xiang, C. Shen, L. Zou and Q. Li, *Foods*, 2022, **11**, 2165.
20 Y.-Y. Yang, Y.-T. Li, X.-J. Li, L. Zhang, E. Kouadio Fodjo and S. Han, *Chem. Eng. J.*, 2020, **402**, 125179.
21 W. Liu, C. Jing, X. Liu and J. Du, *Analyst*, 2022, **147**, 223–229.